Fine-scale ecological and economic assessment of climate change on olive in the Mediterranean Basin reveals winners and losers

Luigi Ponti[a,b,1], Andrew Paul Gutierrez[b,c], Paolo Michele Ruti[d], and Alessandro Dell'Aquila[d]

[a]Laboratorio Gestione Sostenibile degli Agroecosistemi, Agenzia nazionale per le nuove tecnologie, l'energia e lo sviluppo economico sostenibile (ENEA), Centro Ricerche Casaccia, 00123 Rome, Italy; [b]Center for the Analysis of Sustainable Agricultural Systems Global, Kensington, CA 94707; [c]College of Natural Resources, University of California, Berkeley, CA 94720; and [d]Laboratorio Modellistica Climatica e Impatti, Agenzia nazionale per le nuove tecnologie, l'energia e lo sviluppo economico sostenibile (ENEA), Centro Ricerche Casaccia, 00123 Rome, Italy

The Mediterranean Basin is a climate and biodiversity hot spot, and climate change threatens agro-ecosystems such as olive, an ancient drought-tolerant crop of considerable ecological and socio-economic importance. Climate change will impact the interactions of olive and the obligate olive fruit fly (*Bactrocera oleae*), and alter the economics of olive culture across the Basin. We estimate the effects of climate change on the dynamics and interaction of olive and the fly using physiologically based demographic models in a geographic information system context as driven by daily climate change scenario weather. A regional climate model that includes fine-scale representation of the effects of topography and the influence of the Mediterranean Sea on regional climate was used to scale the global climate data. The system model for olive/olive fly was used as the production function in our economic analysis, replacing the commonly used production-damage control function. Climate warming will affect olive yield and fly infestation levels across the Basin, resulting in economic winners and losers at the local and regional scales. At the local scale, profitability of small olive farms in many marginal areas of Europe and elsewhere in the Basin will decrease, leading to increased abandonment. These marginal farms are critical to conserving soil, maintaining biodiversity, and reducing fire risk in these areas. Our fine-scale bioeconomic approach provides a realistic prototype for assessing climate change impacts in other Mediterranean agro-ecosystems facing extant and new invasive pests.

ecological impacts | economic impacts | species interactions | *Olea europaea* | desertification

The Mediterranean Basin is a climate change (1) and biodiversity (2) hot spot where substantial warming is predicted in the next few decades (3). A 2 °C increase in average temperature is a widely used metric for assessing risks associated with global warming and as a policy reference, and this level of warming will likely occur in the Basin between 2030 and 2060 (4) with unknown biological and economic impact on major crop systems. Small differences in average climate warming are predicted for the Basin by A1B and higher greenhouse-gases (GHG) forcing scenarios within the 2050 time horizon (5).

A major agro-ecosystem in the Basin is olive (*Olea europaea* L.), an ancient ubiquitous crop of considerable socioeconomic importance (6). A detailed review of methods used to assess the impact of weather and of climate change on the olive system is given in *SI Appendix*. Most of the crop is used to produce olive oil, with Basin countries producing 97% of the world supply (International Olive Council, www.internationaloliveoil.org/). Olive is a long-lived drought-tolerant species limited by frost and high temperatures, and to a lesser extent by low soil fertility and soil water (7). Temperatures <-8.3 °C damage olive and limit its northward distribution, whereas annual rainfall <350 mm y^{-1} limits its distribution in arid regions. Commercial olive production occurs in areas with >500 mm rainfall y^{-1} (*SI Appendix*, Fig. S1). Climate models predict increased temperatures for the Mediterranean Basin in response to increasing [GHG], but only

a weak negative trend in precipitation and no trend in evaporation are predicted (8). Growth rates in some plants will increase with [CO$_2$] within their thermal and moisture limits (7, 9), but the response for olive is unknown.

Mainstream assessments of climate change impact on agricultural and other ecosystems have omitted trophic interactions (10). Here we include the effects of climate change on olive phenology, growth, and yield, and on the dynamics and impact of its obligate major pest, the olive fruit fly [*Bactrocera oleae* (Rossi)]. The thermal limits of olive and the fly differ and affect the trophic interactions (11) crucial to estimating the bioeconomic impact of climate change in olive across the Basin.

Previous assessments of climate change on heterothermic species have used ecological niche modeling (ENM) approaches that characterize climatically a species' geographic range based on observed aggregate weather data in areas of its recorded distribution (for olive, see, e.g., ref. 12). ENMs are often used to predict the distribution of the species in response to climate change (13) despite serious deficiencies including the inability to include trophic interactions (14). Moreover, the implicit mathematical and ecological assumptions of ENMs hinder biological interpretation of the results (15).

As an alternative we use mechanistic physiologically based demographic models (PBDMs) that explicitly capture the weather-driven biology of interacting species (e.g., ref. 16) and predict the geographic distribution and relative abundance of species across time and space independent of species distribution records using extant and climate change weather scenarios as drivers for the system. The explicit assumptions in PBDMs have heuristic

---

Significance

Inability to determine reliably the direction and magnitude of change in natural and agro-ecosystems due to climate change poses considerable challenge to their management. Olive is an ancient ubiquitous crop having considerable ecological and socioeconomic importance in the Mediterranean Basin. We assess the ecological and economic impact of projected 1.8 °C climate warming on olive and its obligate pest, the olive fly. This level of climate warming will have varying impact on olive yield and fly infestation levels across the Mediterranean Basin, and result in economic winners and losers. The analysis predicts areas of decreased profitability that will increase the risk of abandonment of small farms in marginal areas critical to soil and biodiversity conservation and to fire risk reduction.

Fig. 1. Multitrophic biology of the olive/olive fly system. (*A*) Dry matter flow in olive and to olive fly, and (*B*) dynamics of olive fly number (see ref. 22).

value, and bridge the gap between long run field experiments used to study global change biology and the narrow methodological and conceptual bases of ENM approaches commonly used in macroecology (17, 18). These attributes are essential for assessing the bioeconomic consequences of climate warming on trophic interactions across large landscapes.

Linked PBDMs for olive and olive fly in a geographic information system (GIS) context (11) (Fig. 1 and *SI Appendix*, Fig. S2) are used to estimate the fine-scale ecological and economic impact of climate warming on olive yield and fly infestation across the Basin using baseline daily weather (scenario $\vec{w}_0$) simulated under observed [GHG], and the increasing [GHG] A1B emissions scenario ($\vec{w}_{+1.8}$) of the Intergovernmental Panel on Climate Change (IPCC) (*Materials and Methods* and *SI Appendix, SI Materials and Methods*).

Results

Distribution of Olive. The distribution of olive across the ecological zones of the Mediterranean Basin is illustrated in Fig. 2*A* with the area in each country planted to olive illustrated in *SI Appendix*, Fig. S3 (FAOSTAT data, http://faostat.fao.org/). Inconsistencies were found between the different data sets used to develop a corrected distribution map for olive (see details on data sources in *SI Appendix, SI Materials and Methods*). For example, both Food and Agriculture Organization of the United Nations - Global Agro-Ecological Zones (FAO GAEZ) and M3-Crops data report a very small olive-growing area for the island of Sicily despite its 10% contribution to Italian production (ISTAT, www.istat.it/). The FAO GAEZ spatial data report olive throughout the Po valley in Northern Italy where olive is sparse and with posited yields higher than in the world-leading province of Andalucía, Spain. The distributions of olive in Sicily and the Po Valley were corrected using Corine satellite-based land cover and raw yield data from FAO Agro-MAPS. Furthermore, M3-Crops data show olive plantings in northern Egypt that FAO GAEZ does not report, and both FAO GAEZ and M3-Crops report olive in the central highlands of Turkey where it is largely absent (19).

Our distribution map for olive in the Mediterranean Basin shows that 75% of the cultivation falls within the subtropical dry forest ecological zone (Sdfz) defined by the presence of olive and *Quercus ilex* L (20), 16% falls within the subtropical steppe zone—a transitional zone that separates Sdfz from the Sahara

Desert, and the remaining 9% occurs in marginal ecological zones including colder temperate zones and subtropical mountain ranges, or in deserts under irrigation (Fig. 2*B*).

Simulation of Olive and Fly Dynamics. *Olive.* Using weather scenarios ($\vec{w}_0$ and $\vec{w}_{+1.8}$), the model predicts many aspects of olive and fly dynamics (11) (Fig. 3). As an example, the 10-y dynamics of olive fruit production and olive fly infestation rates are illustrated for Villacidro in the southern part of the island of Sardinia, Italy (latitude: 39.428°N; longitude: 8.881°E) during 1991–2000 (Fig. 3*A*) (21). The fruit and fly dynamics for 1991 are expanded in the stippled area in Fig. 3 *B–D* to show the detailed weather-driven biology computed on a daily basis at all 995 locations across the Mediterranean Basin. The model predicts the dynamics of adult reproductive quiescence and populations (Fig. 3*C*) and of fly immature stage populations in attacked fruit (Fig. 3*D*).

Bloom date is a major factor determining season length and potential yield (7) that the model accurately captured for California, Italy, and Sardinia (11, 21) (*SI Appendix, SI Discussion*). The predictions for the Basin using $\vec{w}_0$ are consistent with field observations (22) (*SI Appendix*, Fig. S4), but using $\vec{w}_{+1.8}$, bloom dates are predicted to occur earlier across the Basin, being up to 18 d earlier in areas of the Iberian Peninsula, North Africa, and Greece (Fig. 4*A*). Mean flowering dates and SD for $\vec{w}_0$ and $\vec{w}_{+1.8}$ scenarios are summarized in *SI Appendix*, Figs. S4 and S5, respectively.

Fig. 2. Geographic distribution of olive as: (*A*) the observed distribution of olive in the Mediterranean Basin (red) superimposed on a shaded relief map with coloring based on satellite-derived land cover from Natural Earth (http://www.naturalearthdata.com/); and (*B*) map of FAO ecological zones (20) included in the domain of the analysis, with the histogram showing the proportion of the total olive area in *A* within the ecological zones. Color palette in *B* is from http://colorbrewer2.org/.
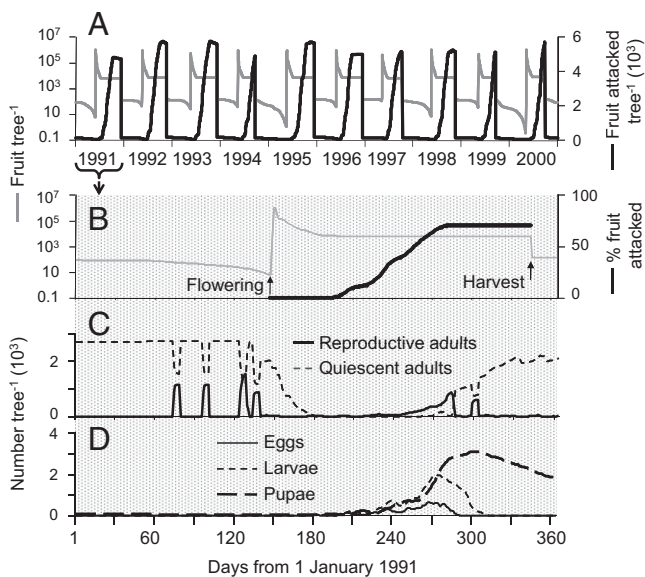
Fig. 3. Example of the simulated phenology of olive and olive fly at each grid point. (*A*) Olive fruiting and olive fly infestation for the period 1991–2000 in a typical olive-growing area near Villacidro in the southern part of Sardinia, Italy (latitude: 39.428°N; longitude: 8.881°E). The fruit and fly dynamics for 1991 are expanded in the stippled area (*B–D*). Plotted data were extracted from a larger simulation for the period 1958–2000 based on daily weather from the ERA40 (reanalysis of meteorological observations from September 1957 to August 2002 produced by the European Centre for Medium-Range Weather Forecasts) climate data downscaled for the Mediterranean region using the Protheus regional climate model (38).

Olive fly. Fly populations are influenced by fruit phenology and abundance, and temperature. Using $\vec{w}_0$, highest fly abundance is predicted in the mild coastal areas of southern Europe and North Africa. The lowest populations are predicted at higher elevations and areas with cold winter weather (e.g., parts of Europe), and in areas where summer temperatures are close to or exceed the fly's upper thermal limits (e.g., the Middle East; see mean and SD in *SI Appendix*, Figs. S6, S7).

With $\vec{w}_{+1.8}$ weather, fly abundance is predicted to increase inland and at higher elevations in Europe that become more favorable for both the plant and fly. Fly populations are predicted to decrease in hotter areas of the Basin as temperatures approach or exceed the upper thermal limits (*SI Appendix*, Fig. S6). The net changes in fly populations in response to climate warming across the Basin are shown in Fig. 4*B*.

Regional Economic Impact of Climate Warming. The net changes in yields, infestation levels, and profit across the Basin are illustrated in Fig. 5, with corresponding changes in their variability illustrated in *SI Appendix*, Fig. S8. Predicted mean yield, infestation level, and profit under $\vec{w}_0$ and $\vec{w}_{+1.8}$ including average change in variability are summarized by Basin subregion (*SI Appendix*, Fig. S9) in Table 1.

The yield order by Basin subregion is not predicted to change with climate warming: Middle East > Greece, Turkey, and the Balkans > France and Italy > Iberian Peninsula > North Africa with yields in most regions except the Middle East increasing (Table 1, Fig. 5*A*). Across the Basin there is a 4.1% increase in total yield and a decrease in yield variability. The predicted yields in North Africa remain low with small increase in variability, whereas in the Middle East yields decline 9.5% and variability increases (*SI Appendix*, Fig. S8).

An average reduction of 8.0% in fly infestation and a small decrease in variability are predicted across the Basin. A 5.9% increase in infestation with reduced variability is predicted in Italy and France, no significant change is predicted for the

Iberian Peninsula, but large declines are predicted in hotter regions of the Middle East and North Africa (Table 1) and Greece, Turkey, and the Balkans (Fig. 5*B*). Largest decreases in variability of infestation are predicted in Turkey and Europe excluding Iberia (*SI Appendix*, Fig. S8).

Changes in profit (ΔΠ) at each location are largely driven by the differing effects of temperature on olive and the fly (*Materials and Methods*). Regional changes in ΔΠ (*Materials and Methods*) are summarized in Table 1 with the net changes on a finer scale depicted in Fig. 5*C*. The order of average change in net profit by Basin subregion is Greece, Turkey, and the Balkans > France and Italy > Iberian Peninsula > North Africa, with ΔΠ being negative in the Middle East (Table 1). In Egypt and most of Israel–Palestine, ΔΠ is negative (Fig. 5*C*) due to decreased yields (Fig. 5*A*) that are not offset by lower infestation levels (Fig. 5*B*), improved oil quality, and reduced control costs (Fig. 5*B*). In contrast, positive ΔΠ accrues in areas of Spain and Italy due to increased yields that offset increased infestation levels, higher control costs, and lower oil quality. ΔΠs decline in northern Portugal and central Spain because of higher infestations levels despite increases in yield. In areas of North Africa, net profits increase despite small reductions in yield because of large reductions in infestation levels, lower control costs, and improved oil quality. As a percentage, the average change in net profit across the Basin is 9.6%, in North Africa it is 41.1%, with only the Middle East showing an average decline of −7.2%.

Overall, the largest average net gains and decreases in variability of yield and profit are predicted in Europe where warming conditions become more favorable for olive, whereas the smallest net gains in profit accrue in North Africa (Fig. 5). However, climate changes will have greater impact on some areas within these regions creating winner and losers (*Discussion*). In the absence of irrigation, olive production in the hottest areas may be further compromised by expected small increases in aridity (8), but this factor was not included in the analysis.
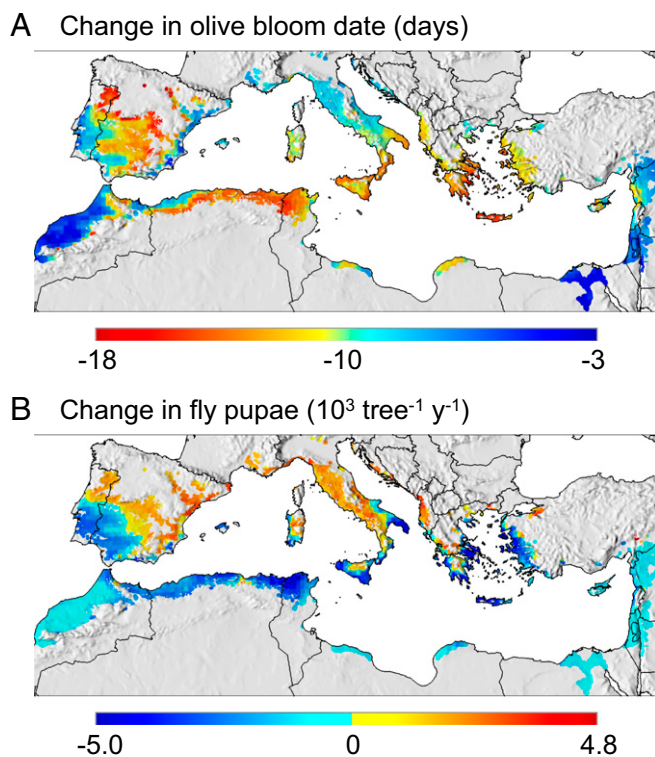

A Change in olive bloom date (days)

-18   -10   -3

B Change in fly pupae (10^3 tree^{-1} y^{-1})

-5.0   0   4.8

Fig. 4. Impact of climate warming on olive phenology and olive fly abundance in the Mediterranean Basin. (*A*) Change in olive bloom date (days) and (*B*) in olive fly abundance (cumulative pupae × 10^3 tree^{-1}·y^{-1}) under the A1B scenario of 1.8 °C climate warming.

A ΔY (change in olive yield, t ha⁻¹)

B ΔI (change in fruit attacked, %)

C ΔΠ (change in profit, € ha⁻¹)

Fig. 5. Bioeconomic multitrophic effects of climate warming on olive and olive fly in the Mediterranean Basin. (A) Predicted changes in olive yield (t ha⁻¹); (B) change in infestation by olive fly (% olive fruit attacked by the fly); and (C) change in profit (€ ha⁻¹) under the A1B +1.8 °C climate warming scenario. Statistical outliers are mapped as such for improving data visualization (*SI Appendix, SI Materials and Methods*) and were identified using the boxplot function in R (see www.r-project.org/). Full data intervals are [−1.5, 2.3] (A) and [−914.7, 3,000.0] (C).

Discussion

How to analyze the tripartite ecological, economic, and social effects of climate change has been vexing and largely unexplored. Here we examine these different factors, albeit with different levels of precision.

The recent ecological literature emphasizes the urgent need for alternative approaches for estimating climate change impacts on biological systems such as olive (e.g., ref. 17) (*SI Appendix, SI Discussion*). Widely used ENM correlative approaches have important shortcomings (IPCC, www.ipcc.ch/publications_and_data/ar4/wg2/en/ch4.html) recognized early (23) that stimulated the development of the PBDM approach used here. Other approaches have attempted to integrate physiological mechanisms and population processes in climate impact assessments (*SI Appendix, SI Discussion*), but they remain substantially close to the correlative end of the process-correlation model continuum (24). The PBDM approach explicitly captures the mechanistic weather-driven biology and trophic dynamics in a realistic manner, while keeping model complexity to a minimum. This occurs by applying the same dynamics model and process submodels at all trophic levels (25, 26).

PBDMs have heuristic and predictive value, and have been used in a wide range of successful applications in agro-ecosystem management without transferability issues (e.g., ref. 26) (*SI Appendix, SI Discussion*). The linked PBDMs for olive and olive fly gave heuristic insights and good predictions of the spatiotemporal patterns of olive phenology and yield, and robust predictions about the geographic distribution and relative abundance of olive fly across large geographic areas of North America (26), Italy, and Sardinia (11, 21). The models were used here in a bioeconomic analysis of the effects of climate change on olive and the fly in the Mediterranean Basin.

The Basin has a wide diversity of olive culture systems, local varieties, and agronomic practices, but there is a dearth of suitable data for model parameterization and testing (*SI Appendix, SI Discussion*). These factors make precise prediction of yield across these olive systems an unrealistic goal. To circumvent these limitations, observed average yield data for the reference period 1997–2003 that implicitly include the effects of local agronomic practices and varieties (*SI Appendix, Fig. S10*) were scaled by normalized PBDM predictions of the metaphysiological response of olive to $\vec{w}_0$ and

Table 1. Mean values for olive yield, olive fly infestation, and profit in the different subregions of the Mediterranean Basin (see map of subregions in *SI Appendix, Fig. S9*) for years 1961–1970 under the baseline climate scenario ("base") and for years 2041–2050 under the A1B scenario of 1.8 °C climate warming

Zone	Olive yield, t ha⁻¹			Olive fly infestation, % fruit infested			Profit, € ha⁻¹		
	Obs.	A1B	ΔCV	Base	A1B	ΔIQR	Base	A1B	ΔIQR
Portugal, Spain	1.51	1.71***	−9.9	50.7	51.4	0.4	674.3	790.3***	−16.3
France, Italy	2.14	2.37***	−11.4	58.7	64.6***	−5.6	2,179.0	2,398.0***	−111.6
Croatia, Albania, Greece, Turkey, Cyprus	2.20	2.38***	−23.1	57.8	45.5***	−5.8	2,235.0	2,491.1***	−168.9
Egypt, Israel, Palestine, Jordan, Lebanon, Syria	3.40	3.08***	3.8	31.2	16.7***	−0.3	1,789.7	1,661.3***	94.1
Morocco, Algeria, Tunisia, Libya	1.22	1.23	1.2	47.7	28.5***	0.3	209.6	295.8***	3.7
Overall Basin	1.88	1.96***	−6.9	49.6	41.5***	−1.6	1,161.5	1,272.8***	−32.9

Welch's two-sample t test for A1B vs. observed or baseline: *** for $P < 0.001$ otherwise $P \geq 0.05$. "Obs." stands for observed yields (i.e., Y_{obs}). Mean changes in variability resulting from climate warming in the different subregions are indicated for yield as the difference in the coefficient of variation ($\Delta CV = CV_{+1.8} - CV_0$), and for olive fly infestation and profit as the difference in the interquartile range ($\Delta IQR = IQR_{+1.8} - IQR_0$) (*SI Appendix, SI Materials and Methods*).

$\vec{w}_{+1.8}$ weather scenarios at each grid point across the Basin (*Materials and Methods*). The combination of observed and simulated data was used as the production function (27) in our analysis to estimate the effects of climate change on changes in yield, profit, pest control costs, and quality of olives. An important factor in the analysis is that olive and olive fly have different tolerances to temperature (see figure 1 in ref. 11) that greatly affect their interactions and the economics of olive production across the Basin.

Average climate warming of 1.8 °C will benefit some olive-producing areas, adversely affect others, and some will remain relatively unchanged. Comparing the periods 1961–1970 and 2041–2050, the models predict minimal impact of climate warming on aggregate olive oil production with some decrease in risk across the Basin. However, on a finer scale, the economic impact is not uniform. The percentages of the olive-growing area in each subregion with predicted declines in net profit are 18% for the Iberian Peninsula, 21% for Italy and France, 23% for Greece, Turkey, and the Balkans, 2% for North Africa, and 80% for the Middle East (see regional histograms in Fig. 6 and Table 1; see variability measures in *SI Appendix*, Fig. S8). These are important changes because olive culture has historically played an important role in rural development and poverty alleviation in marginal areas across the Middle East and North Africa (28) and parts of Europe (29).

High economic losses in Italy, Greece, and the Middle East are expected on small olive farms in marginal areas common on sloping lands, with the impact being greatest in areas prone to desertification (30) (*SI Appendix, SI Discussion*). Exacerbating the problem is that increases in fly infestation levels in some areas would increase insecticide use and the development of resistance (31), and associated increased costs and losses. However, data to model these aspects are not available. In the European Union (EU), the viability of small farms will be further compromised by subsidy policies that favor intensive, less ecologically sustainable olive production systems (29) (*SI Appendix, SI Discussion*). The combined effect of climate warming and economic EU policy will increase the rate of abandonment of at-risk farms (32) that in addition to income, provide important ecosystem services such as soil conservation, biodiversity habitat, and wildfire prevention (29, 30) (*SI Appendix, SI Discussion*). Technology changes may occur to mitigate climate change effects in some areas (e.g., irrigation), but data are unavailable to include this in our analysis. We note that the limits on olive imposed by increased respiration due to higher temperature would not be removed by irrigation.
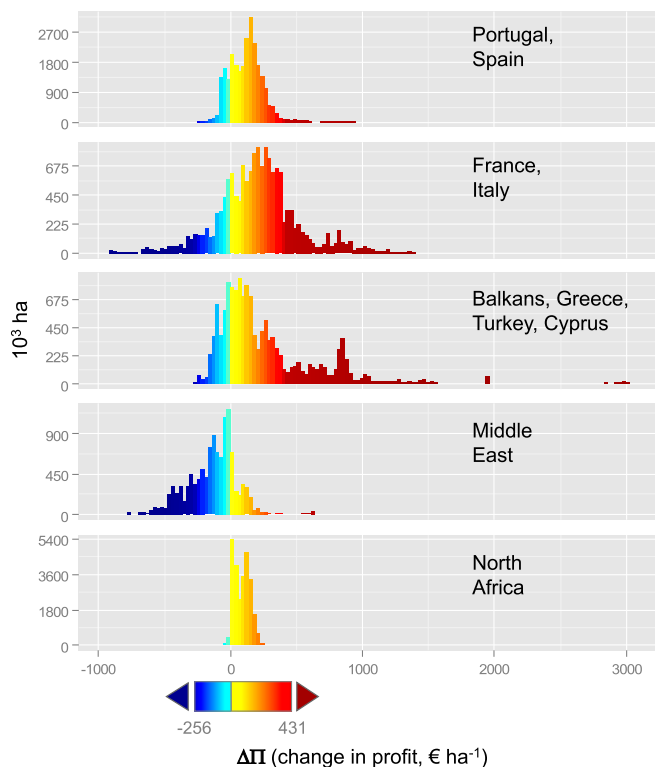
The analysis demonstrates the importance of including trophic interactions in assessing biological and economic impacts of climate change over large geographic areas, and provides a template for assessing climate change impact in other agro-ecosystems (e.g., grape, citrus, etc.) in the face of extant and potentially new invasive pests (33, 34). The ecological and bioeconomic effects of climate warming are expected to be far greater on more heat- and drought-intolerant crops such as grape and wheat (4, 35), and especially in areas that will experience increased aridity (8).

Materials and Methods

The System Model. The underlying assumption of the models is that all organisms in all trophic levels, including the economic one, are consumers that have similar resource acquisition (inputs) and allocation (outputs) priorities (25, 36, 37). Based on analogies, the dynamics of olive and olive fly were captured using the same resource acquisition and birth–death rate submodels imbedded in an age-mass structured population model (PBDM) (*SI Appendix, Mathematical Structure of the Olive/Olive Fly Model*). Resource acquisition (i.e., the supply, S) is a search process driven by organism demand (D), whereas allocation occurs in priority order to egestion, conversion costs, respiration, and reproduction, growth, and reserves. The ratio $0 \leq S/D < 1$ is due to imperfect consumer search, and in the model scales maximal growth rates of the species in a time–place varying manner. At high resource levels, $S/D \rightarrow 1$. The model for olive is a canopy model with subunit populations of leaves, stem, root, and healthy and attacked fruit. The model simulates the age-mass structured population dynamics of plant subunits and of olive fly numbers (11). The olive model predicts flowering phenology controlled by vernalization, the age-structured dynamics of growth and yield, and fruit mortality due to temperature and fly attack. Olive fly biology is closely linked to olive fruit phenology, age, and abundance. The effects of temperature on vital rates of olive fruit and the fly are captured by normalized concave scalar functions that approximate the net of S corrected for metabolic costs across temperature (11).

Weather to drive the plant–fly dynamics includes daily maximum and minimum temperatures and solar radiation for years 1960–1970 and 2040–2050 from a global climate model simulation for the period 1951–2050 (8). The first 50 y of the weather data were based on observed GHG concentration, and the second 50 were based on the A1B GHG scenario of the IPCC Special Report on Emissions Scenarios. The global climate simulation was downscaled via the Protheus regional climate model (38). Geographic resources analysis support system (GRASS) GIS (http://grass.osgeo.org/) was used to perform geospatial analysis and produce maps.

The Bioeconomic Model. To assess economic benefit in agriculture, economists commonly use the production and damage control function approaches (27, 39, 40), but here we use the PBDM for the olive system as the production function using weather scenarios $\bar{w}_0$ and $\bar{w}_{+1.8}$ as the drivers (*SI Appendix, Mathematical Structure of the Olive/Olive Fly Model*). The model predicts considerable biological detail (see Fig. 3 for the dynamics of a sample location), but only yield tree^{-1} [$Y_0 = f(\bar{w}_0, P_0)$ and $Y_{+1.8} = f(\bar{w}_{+1.8}, P_{+1.8})$], cumulative fly pupae tree^{-1}y^{-1} [$P_0 = g(\bar{w}_0, Y_0)$ and $P_{+1.8} = g(\bar{w}_{+1.8}, Y_{+1.8})$], and percentage infested fruit in the absence of pest control [$I_0 = h(\bar{w}_0, Y_0, P_0)$ and $I_{+1.8} = h(\bar{w}_{+1.8}, Y_{+1.8}, P_{+1.8})$] are used as metrics of system performance (27, 37). The net simulated change in yield due to climate warming at a grid point is $\Delta Y = Y_{+1.8} - Y_0$, and when divided by the maximum difference ($\Delta Y_{max} - \Delta Y_{min}$) across all locations predicts the relative change in yield at each location (Eq. 1).

$$Y_{index} = \left(\frac{Y_{+1.8} - Y_0}{\Delta Y_{max} - \Delta Y_{min}} \right). \qquad [1]$$

However, to correct for the effects of variety, plant age structure, and agronomic practices that affect yield, we multiplied Y_{index} by the observed average yield ha^{-1} (Y_{obs}) at each location during the period 1997–2003 (*SI Appendix*, Fig. S10; ref. 41) (Eq. 2).

Fig. 6. Frequency distribution of net economic gains and losses in olive due to climate warming. Histograms illustrate the frequency distribution of net profit gains and losses in different subregions of the Mediterranean Basin (see maps of subregions in *SI Appendix*, Fig. S9). Change in profit values in histograms is mapped to color as in Fig. 5C.

$$\Delta Y = Y_{obs} \cdot Y_{index}. \qquad [2]$$

Furthermore, because most of the olive harvest is used for oil production, ΔY is converted to liters of oil by multiplying by a country-specific factor (θ) based on FAO data for the year 2000 (http://faostat.fao.org/).

To compute the net change in profit ($\Delta\Pi$) (Eq. **3**), we must include both the change in quality and price with changes in % infestation levels (I), and control costs.

$$\Delta\Pi = \theta \cdot \Delta Y \cdot \hat{p}_0(I) - \Delta n \cdot p_x. \qquad [3]$$

The price of oil (p_0) declines with I [i.e., $\hat{p}_0(I) = p_0 e^{-\alpha I}$], where $\alpha = 0.5$ decreases the price to 40% at $I = 100\%$ (42). The cost of pest control is $\Delta n \cdot p_x$, where p_x (50€ ha^{-1}) is the cost per application of insecticide (43), and Δn is the change in the number of applications with I. The number of applications at a location increases linearly from an infestation threshold of $I_{th} = 4\%$ (44) to a maximum $n = 7$ at $I_{max} = 85\%$ (45). The net change in the number of applications (Δn) (Eq. **4**) is computed as a function of the net change in infestation level with climate warming (i.e., $\Delta I = I_{+1.8} - I_0$) (e.g., ref. 43).

$$\Delta n = 7 \cdot \left(\frac{\Delta I}{I_{max} - I_{th}} \right). \qquad [4]$$

Note that if ΔI is positive, $\Delta n \cdot p_x$ increases and $\hat{p}_0(I)$ decreases, and if negative the reverse occurs. Furthermore, key to understanding the results of the analysis is that olive has a higher range of tolerance to temperature than olive fly (see figure 1 in ref. 11), and the price penalty on infested olives used for oil production is relatively low.

The model ignores changes in market-induced prices that may occur as a result of climate-driven spatial and temporal shifts in olive production. Currently, supply effects mostly occur at the country level, whereas the quality of oil remains an important determinant of oil price across the Basin (see http://ec.europa.eu/agriculture/olive-oil/economic-analysis_en.pdf and *SI Appendix, SI Discussion*). Agricultural policy has influenced olive oil production and price across the Basin, and especially via substantial subsidies in the EU briefly outlined in *SI Appendix, SI Discussion*.

1. Giorgi F (2006) Climate change hot-spots. *Geophys Res Lett* 33(8):L08707.
2. Myers N, Mittermeier RA, Mittermeier CG, da Fonseca GAB, Kent J (2000) Biodiversity hotspots for conservation priorities. *Nature* 403(6772):853–858.
3. Gualdi S, et al. (2013) The CIRCE simulations: A new set of regional climate change projections performed with a realistic representation of the Mediterranean Sea. *Bull Am Meteorol Soc* 94(1):65–81.
4. Giannakopoulos C, et al. (2009) Climatic changes and associated impacts in the Mediterranean resulting from a 2 °C global warming. *Global Planet Change* 68(3):209–224.
5. Giorgi F, Bi X (2005) Updated regional precipitation and temperature changes for the 21st century from ensembles of recent AOGCM simulations. *Geophys Res Lett* 32(21):L21715.
6. Loumou A, Giourga C (2003) Olive groves: "The life and identity of the Mediterranean. *Agric Human Values* 20(1):87–95.
7. Connor DJ, Fereres E (2005) The physiology of adaptation and yield expression in olive. *Hortic Rev (Am Soc Hortic Sci)* 31:155–229.
8. Dell'Aquila A, et al. (2012) Effects of seasonal cycle fluctuations in an A1B scenario over the Euro-Mediterranean region. *Clim Res* 52:135–157.
9. Morison JIL, Lawlor DW (1999) Interactions between increasing CO$_2$ concentration and temperature on plant growth. *Plant Cell Environ* 22(6):659–682.
10. Van der Putten WH, Macel M, Visser ME (2010) Predicting species distribution and abundance responses to climate change: Why it is essential to include biotic interactions across trophic levels. *Philos Trans R Soc Lond B Biol Sci* 365(1549):2025–2034.
11. Gutierrez AP, Ponti L, Cossu QA (2009) Effects of climate warming on olive and olive fly (*Bactrocera oleae* (Gmelin)) in California and Italy. *Clim Change* 95(1-2):195–217.
12. Moriondo M, et al. (2013) Olive trees as bio-indicators of climate evolution in the Mediterranean Basin. *Glob Ecol Biogeogr* 22(7):818–833.
13. Pearson RG, Dawson TP (2003) Predicting the impacts of climate change on the distribution of species: Are bioclimate envelope models useful? *Glob Ecol Biogeogr* 12(5):361–371.
14. Zarnetske PL, Skelly DK, Urban MC (2012) Ecology. Biotic multipliers of climate change. *Science* 336(6088):1516–1518.
15. Soberón J, Nakamura M (2009) Niches and distributional areas: Concepts, methods, and assumptions. *Proc Natl Acad Sci USA* 106(Suppl 2):19644–19650.
16. Gutierrez AP, Pitcairn MJ, Ellis CK, Carruthers N, Ghezelbash R (2005) Evaluating biological control of yellow starthistle (*Centaurea solstitialis*) in California: A GIS based supply-demand demographic model. *Biol Control* 34(2):115–131.
17. Dawson TP, Jackson ST, House JI, Prentice IC, Mace GM (2011) Beyond predictions: Biodiversity conservation in a changing climate. *Science* 332(6025):53–58.
18. Kerr JT, Kharouba HM, Currie DJ (2007) The macroecological contribution to global change solutions. *Science* 316(5831):1581–1584.
19. Işk N, Doğanlar S, Frary A (2011) Genetic diversity of Turkish olive varieties assessed by simple sequence repeat and sequence-related amplified polymorphism markers. *Crop Sci* 51(4):1646–1654.
20. FAO, Food and Agriculture Organization of the United Nations (2001) *Global Ecological Zoning for the Global Forest Resources Assessment 2000: Final Report. Working Paper 56* (FAO, Rome).
21. Ponti L, Cossu QA, Gutierrez AP (2009) Climate warming effects on the *Olea europaea–Bactrocera oleae* system in Mediterranean islands: Sardinia as an example. *Glob Change Biol* 15(12):2874–2884.
22. Orlandi F, et al. (2010) Olive flowering trends in a large Mediterranean area (Italy and Spain). *Int J Biometeorol* 54(2):151–163.
23. Gutierrez AP, Nix HA, Havenstein DE, Moore PA (1974) The ecology of *Aphis craccivora* Koch and subterranean clover stunt virus in south-east Australia. III. A regional perspective of the phenology and migration of the cowpea aphid. *J Appl Ecol* 11(1):21–35.
24. Dormann CF, et al. (2012) Correlation and process in species distribution models: Bridging a dichotomy. *J Biogeogr* 39:2119–2131.
25. Gutierrez AP, Mills NJ, Schreiber SJ, Ellis CK (1994) A physiologically based tritrophic perspective on bottom-up-top-down regulation of populations. *Ecology* 75(8):2227–2242.
26. Gutierrez AP, Ponti L (2013) Eradication of invasive species: Why the biology matters. *Environ Entomol* 42(3):395–411.
27. Pemsl DE, Gutierrez AP, Waibel H (2008) The economics of biotechnology under ecosystem disruption. *Ecol Econ* 66(1):177–183.
28. Lybbert TJ, Elabed G (2013) An elixir for development? Olive oil policies and poverty alleviation in the Middle East and North Africa. *Dev Policy Rev* 31(4):485–506.
29. Fleskens L, de Graaff J (2010) Conserving natural resources in olive orchards on sloping land: Alternative goal programming approaches towards effective design of cross-compliance and agri-environmental measures. *Agric Syst* 103(8):521–534.
30. Duarte F, Jones N, Fleskens L (2008) Traditional olive orchards on sloping land: Sustainability or abandonment? *J Environ Manage* 89(2):86–98.
31. Skouras PJ, et al. (2007) Organophosphate resistance in olive fruit fly, *Bactrocera oleae*, populations in Greece and Cyprus. *Pest Manag Sci* 63(1):42–48.
32. de Graaff J, Duarte F, Fleskens L, De Figueiredo T (2010) The future of olive groves on sloping land and ex-ante assessment of cross compliance for erosion control. *Land Use Policy* 27(1):33–41.
33. Moriondo M, Bindi M, Fagarazzi C, Ferrise R, Trombi G (2011) Framework for high-resolution climate change impact assessment on grapevines at a regional scale. *Reg Environ Change* 11(3):553–567.
34. Caffarra A, Eccel E (2011) Projecting the impacts of climate change on the phenology of grapevine in a mountain area. *Aust J Grape Wine Res* 17(1):52–61.
35. Quiroga S, Iglesias A (2009) A comparison of the climate risks of cereal, citrus, grapevine and olive production in Spain. *Agric Syst* 101(1–2):91–100.
36. Gutierrez AP (1996) *Applied Population Ecology: A Supply-Demand Approach* (Wiley, New York).
37. Regev U, Gutierrez AP, Schreiber SJ, Zilberman D (1998) Biological and economic foundations of renewable resource exploitation. *Ecol Econ* 26(3):227–242.
38. Artale V, et al. (2010) An atmosphere-ocean regional climate model for the Mediterranean area: Assessment of a present climate simulation. *Clim Dyn* 35(5):721–740.
39. Cobourn KM, Burrack HJ, Goodhue RE, Williams JC, Zalom FG (2011) Implications of simultaneity in a physical damage function. *J Environ Econ Manage* 62:278–289.
40. Lichtenberg E, Zilberman D (1986) The econometrics of damage control: Why specification matters. *Am J Agric Econ* 68(2):261–273.
41. Monfreda C, Ramankutty N, Foley JA (2008) Farming the planet: 2. Geographic distribution of crop areas, yields, physiological types, and net primary production in the year 2000. *Global Biogeochem Cycles* 22(1):GB1022.
42. Haniotakis GE (2005) Olive pest control: Present status and prospects. *IOBC WPRS Bull* 28(9):1–9.
43. Gilioli G, Cossu QA, Zinni A (2005) Un modello di simulazione per la difesa dalla mosca delle olive in Abruzzo. II. Aspetti economici e di impatto ambientale. *Ital J Agromet* 1:18–19.
44. Viggiani G (1989) La difesa integrata dell'olivo: Attualità e prospettive. *Inf Fitopatol* 2:23–32.
45. Collier TR, van Steenwyk RA (2003) Prospects for integrated control of olive fruit fly are promising in California. *Calif Agric* 57(1):28–30.

ECONOMIC SCIENCES

ECOLOGY